

Dipole Instability of a Relativistic
Electron Ring Loaded With
Two Species of Ions

W. Ott, W. Dommaschk and E. Springmann

IPP O/23

July 1974

MAX-PLANCK-INSTITUT FÜR PLASMAFYSIK
GARCHING BEI MÜNCHEN

Dipole Instability of a
MAX-PLANCK-INSTITUT FÜR PLASMA PHYSIK
GARCHING BEI MÜNCHEN

Dipole Instability of a Relativistic
Electron Ring Loaded With
Two Species of Ions

W. Ott, W. Dommaschk and E. Springmann

IPP O/23

July 1974

*Die nachstehende Arbeit wurde im Rahmen des Vertrages zwischen dem
Max-Planck-Institut für Plasmaphysik und der Europäischen Atomgemeinschaft über die
Zusammenarbeit auf dem Gebiete der Plasmaphysik durchgeführt.*

IPP 0/23

W. Ott
W. Dommaschk
E. Springmann

Dipole Instability of a
Relativistic Electron
Ring Loaded with two
Species of Ions

July 1974

Abstract

The electrostatic interaction of a relativistic electron ring with the ions contained in it leads to instability under certain conditions, as is well known. Since there are always different ion species present in the ring, the influence of the ion mixture on the instability is investigated in this paper. A dispersion equation is derived in which, besides the interaction of the electrons with one ion species, both the collective interaction of the electrons with a second ion species and the collective interaction between the two ion species are taken into account. As solutions of these equations show, no excessive enhancement or suppression of the instability nor an appreciable displacement of the region of instability due to the additional interaction takes place. For sufficiently small fractional ion loading the region of instability splits into two regions corresponding to the separate interactions of each ion species with the electrons.

The instability of an electron ring arising from its interaction with ions contained in it was treated in several papers theoretically ¹⁾²⁾³⁾ and experimentally ⁴⁾. In Ref. 5 the additional focussing effects which result from cylindrical structures like a "squirrel cage" inside or outside the ring were included in the theory. The present treatment extends this theory to the interaction of the electron ring with two kinds of ions. This same question was dealt with by Nikolaeva and Koshkarev ⁶⁾. In their paper, however, the interaction among the ions was neglected. Their treatment is therefore valid only for small fractional ion loading. Furthermore the magnetic field effect on the ion motion is neglected there which becomes important for the radial instability when the resonance frequencies become very small.

Derivation of the dispersion equation

The equations of radial motions for the electrons and the two kinds of ions are

$$\left. \begin{aligned} \frac{1}{\omega_0^2} \ddot{r}_e &= -q_e^2 r_e + q_{e1}^2 r_1 + q_{e2}^2 r_2 \\ \frac{1}{\omega_0^2} \ddot{r}_1 &= q_{1e}^2 r_e - q_{11}^2 r_1 - q_{12}^2 r_2 \\ \frac{1}{\omega_0^2} \ddot{r}_2 &= q_{2e}^2 r_e - q_{21}^2 r_1 - q_{22}^2 r_2 \end{aligned} \right\} \quad (1)$$

where r_e , r_1 and r_2 are collective radial displacements and ω_0 is the electron revolution frequency. The q 's can be written in analogy to Ref. 5:

$$\left. \begin{aligned}
 q_e^2 &= 1 - n + \rho \left(f_1 + f_2 - \frac{1}{2\alpha_E^2} + \frac{\beta^2}{2\alpha_M^2} \right) \\
 q_{e1}^2 &= \rho f_1 \left(1 - \frac{1}{4\alpha_E^2} \right) \\
 q_{e2}^2 &= \rho f_2 \left(1 - \frac{1}{4\alpha_E^2} \right) \\
 q_1^2 &= \rho Q_{g1} \left(1 - f_2 - \frac{f_1}{2\alpha_E^2} \right) + Q_{g1}^2 \\
 q_{12}^2 &= \rho f_2 Q_{g1} \left(1 - \frac{1}{4\alpha_E^2} \right) \\
 q_{1e}^2 &= \rho Q_{g1} \left(1 - \frac{1}{4\alpha_E^2} \right) \\
 q_2^2 &= \rho Q_{g2} \left(1 - f_1 - \frac{f_2}{2\alpha_E^2} \right) + Q_{g2}^2 \\
 q_{21}^2 &= \rho f_1 Q_{g2} \left(1 - \frac{1}{4\alpha_E^2} \right) \\
 q_{2e}^2 &= \rho Q_{g2} \left(1 - \frac{1}{4\alpha_E^2} \right)
 \end{aligned} \right\} \quad (2)$$

with

$$\alpha_{E,M} = (R_{E,M} - R) / \sqrt{a \bar{b}}$$

β = electron speed/light speed

$$\gamma = (1 - \beta^2)^{-1/2}$$

$R_{E,M}$ = radius of electric and magnetic images

n = field index = $-(R/B) \cdot (\partial B_z / \partial R)$

$$Q_{g1,2} = z_{1,2} \gamma^{m_e} / m_{i1,2}$$

$$\rho = r_0 R N_e / (\pi a \bar{b} \gamma)$$

$r_0 = 2.82 \cdot 10^{-15} \text{ m}$ = classical electron radius

R = major radius of the electron ring

a = radial half width of minor ring dimension

b = corresponding axial half width

$$\bar{b} = (a + b) / 2$$

$$f_{1,2} = z_{1,2} \cdot N_{1,2} / N_e = \text{fractional ion loadings}$$

The coefficients (2) are valid only in the limit of small curvature of the ring as well as the walls. A better approximation done by I. Hofmann⁷⁾ contains also terms proportional to $\frac{1}{\alpha^E}$. We thought, however, that for our purpose the simpler^E coefficients (2) are good enough.

The set of equations (1) is solved as usual by the assumption

$$r_{e,1,2} \sim \exp [i(m\varphi - \omega t)]$$

where m is the azimuthal mode number, the azimuthal position of the particles taken as being constant for the ions and t for the electrons so that

$$\ddot{r}_e = - (m \omega_0 - \omega)^2 r_e$$

$$\ddot{r}_1 = - \omega^2 r_1$$

$$\ddot{r}_2 = - \omega^2 r_2$$

The equations (1) are reduced to a system of three linear homogenous equations for $r_{e,1,2}$ (with $\vartheta = \omega/\omega_0$):

$$\left. \begin{aligned} [q_e^2 - (m-\vartheta)^2] r_e - q_{e1}^2 r_1 - q_{e2}^2 r_2 &= 0 \\ - q_{1e}^2 r_e + (q_1^2 - \vartheta^2) r_1 + q_{12}^2 r_2 &= 0 \\ - q_{2e}^2 r_e + q_{21}^2 r_1 + (q_2^2 - \vartheta^2) r_2 &= 0 \end{aligned} \right\} \quad (3)$$

Equations (3) have a nonzero solution only if the determinant of the coefficients of $r_{e,1,2}$ is zero.

This leads to the following sixth order equation in v :

$$\begin{aligned} v^6 - 2mv^5 - (q_e^2 + q_1^2 + q_2^2 - m^2)v^4 + 2m(q_1^2 + q_2^2)v^3 \\ + [q_e^2 q_1^2 + q_1^2 q_2^2 + q_2^2 q_e^2 - q_{e1}^2 q_{1e}^2 - q_{12}^2 q_{21}^2 - q_{e2}^2 q_{2e}^2 - m^2(q_1^2 + q_2^2)]v^2 \\ + 2m(q_{12}^2 q_{21}^2 - q_1^2 q_2^2) \cdot v \\ - q_e^2 q_1^2 q_2^2 - q_{e1}^2 q_{12}^2 q_{2e}^2 - q_{e2}^2 q_{1e}^2 q_{21}^2 + q_e^2 q_{12}^2 q_{21}^2 + q_2^2 q_{e1}^2 q_{1e}^2 + q_1^2 q_{e2}^2 q_{2e}^2 \\ - m^2(q_{12}^2 q_{21}^2 - q_1^2 q_2^2) = 0 \end{aligned} \quad (4)$$

A program was written which determines whether all six roots of this equation are real or not and which calculates the highest growth rate in case of complex roots.

Influence of ion mixtures on the instability

In the following we want to get an answer to our main question: Does the mixture of different ion species damp the instability or not? Therefore the growth rate of the instability is calculated for various conditions.

The presentation of the data is similar to LASLETT's⁸⁾: The quantities for the electron ring are kept constant (and taken as they are typically measured in the Garching SCHUKO electron ring experiment):

$$N_e = 5 \cdot 10^{12} \quad \gamma = 27 \quad R = 2,3 \text{ cm}$$

$$a = 0,3 \text{ cm} \quad b = 0,3 \text{ cm} \quad R_{\text{Squi}} = 1,55 \text{ cm}$$

The growth rate is determined in a plane of the two parameters: field index n and sum of the two ion loadings $f = f_1 + f_2$. Like in the more usual $Q_1 - Q_i$ - diagrams there is a cusp of the instability area in the $f - n$ -plane for $f \rightarrow 0$. The n -value of this cusp was given by LASLETT⁸⁾:

$$n_{c,2} = 2\sqrt{(\rho + Q_{g1,2})Q_{g1,2}} - (\rho + Q_{g1,2})Q_{g1,2} - \frac{1}{2}\beta\left(\frac{1}{\alpha_E^2} - \frac{\beta^2}{\alpha_H^2}\right) \quad (5)$$

the limited holding power of the ring during acceleration.

The increase of the ring quality seems therefore necessary. Tab. 1 a,b,c present this critical n-value for three different cases of electron ring quality as a function of the ion mass and the radius of the "squirrel cage". According to Tab. 1 a,b,c it would be possible to avoid the instability by shifting this cusp to negative n-values which is done by using heavy ions and a strong squirrel cage action.

The following tables show the unstable parameter areas in the f-n-plane. The upper halves of the tables give the real part of the complex frequency (or a zero if all solutions of equations 3 are real), the lower halves give the imaginary part. In case of more than one pair of complex conjugate solutions the most unstable case is selected. The critical field index n_c as calculated from equation 5 is indicated at the bottom of each table. In both halves of the tables not the values of the frequencies themselves but their logarithms are printed out according to the relation

$$\text{Printed value} = \text{INTEGER}(100 + 10 \lg(\omega_{r,i}/\omega_0)).$$

To see whether the ion mixture reduces the growth of the instability it is thought of as a gedanken experiment: Without changing any other parameters the field index n is changed at a constant rate. As a relative measure for the total amplitude growth when the susp is crossed we use the approximate expression $\Delta n \sum \omega_i(n) \propto \int \omega_i(t) dt$ although this applies only under rather stringent conditions (sufficiently small values of ω_r , ω_i and sufficiently constant ratios of r_1/r_e and r_2/r_e). To get the above expression the imaginary parts are summed up in horizontal rows of these tables, multiplied with the step width Δn and printed in the last columns, also in a logarithmic form as above.

We choose three examples:

1. A mixture of N_2^+ and N_2^{+2} to see if something extraordinary might happen when different kinds of ions of the same gas are present (Tab. 2a,b,c, and 3a,b,c). This corresponds to the situation in a "waiting room" with different ionization states of the same ions.
2. A mixture $^{14}N^+$ and $^{16}O^+$ to see a possible stabilizing effect of similar charge to mass ratios (Tab. 4a,b,c, and 5a,b,c).
3. A mixture of H^+ and O^{+2} to see whether harmonic resonances occur between the ions (Tab. 6a,b,c, and 7a,b,c).

Discussion

The comparison of the tables for single species and their mixtures shows no stabilizing effect of the mixing of masses. In order to clarify this point further some selected data of Tab. 2 to 7 are collected to Tab. 8 where some numbers for the growth of the instability are rewritten. Tab. 8 clearly shows that the mixture of different ions does not stabilize the electron-ion ring against the dipole instability¹⁰⁾. The table shows that the instability growth is the bigger the lighter the ions (compared for same fractional loading). For a loading of 2% for example the growth for H^+ ions is about 5 times the growth for N_2^+ ions, and about twice the growth for He^+ ions. So a method to make the instability less dangerous would be the use of heavier ions. This is the same conclusion as drawn above concerning the position of the critical field index. The use of heavy ions (or better: ions with a small charge to mass ratio) is impractical, however, because of the large increase in the core voltage. There is a limit of the instability area in the $f - n$ plane for a given value of the core voltage given by LASIETT

the limited holding power of the ring during acceleration. The increase of the ring quality seems therefore necessary not only for a higher holding power but also for suppression of the electron ion resonances.

Acknowledgement

Fruitful discussions with C. Andelfinger, A. Faltens, I. Hofmann and A. Schlüter are gratefully acknowledged.

References

1. F.E. MILLS, Symposium on Electron Ring Accelerators, UCRL-18103, Feb. 1968, p. 448
2. D.G. KOSHKAREV and P.R. ZENKEVICH, Particle Accelerators 3, 1 (1972)
3. W. DOMMASCHK, MPI für Plasmaphysik, Garching, Report IPP O/19 (Dec. 1973)
4. C. ANDELFINGER et al., 9th Int. Conf. on High Energy Accelerators, May 1974, Stanford, Cal., USA
5. W. OTT and L.J. LASLETT, ERAN 234 (March 1974)
6. L.P. NIKOLAEVA and D.G. KOSHKAREV, On three-component electron-ion rings, Report No. ITEP-79, 1973
7. I. HOFMANN, private communication
8. Appendix of Ref. 5
9. Formula (A-8; b) in Ref. 5
10. L.J. LASLETT came to a similar result:
that the resonances arising, in the region of small ion loading, may be rather precisely accounted for by the superposition of resonant regions obtained by considering just one ion species to be present at one time.

ELEKTRONENZAHL, GAMMA: 5.000D 12 2.700D 01
 RINGOMETRIE: R, a, b (CM): 2.300D 00 3.000D-01 3.000D-01
 RHO = 4.245D-01

squirrel cage
 radius (cm)

	1	2	4	8	16	32	64	128	256
4.00	0.1477	0.1029	0.0712	0.0486	0.0326	0.0212	0.0131	0.0073	0.0033
3.95	0.1473	0.1025	0.0708	0.0482	0.0322	0.0208	0.0127	0.0069	0.0029
3.90	0.1468	0.1021	0.0703	0.0478	0.0317	0.0203	0.0122	0.0065	0.0024
3.85	0.1463	0.1016	0.0698	0.0473	0.0312	0.0198	0.0117	0.0060	0.0019
3.80	0.1458	0.1011	0.0693	0.0467	0.0307	0.0193	0.0112	0.0055	0.0014
3.75	0.1452	0.1005	0.0687	0.0461	0.0301	0.0187	0.0106	0.0049	0.0008
3.70	0.1445	0.0998	0.0681	0.0455	0.0294	0.0180	0.0099	0.0042	0.0001
3.65	0.1438	0.0991	0.0673	0.0447	0.0287	0.0173	0.0092	0.0035	-0.0006
3.60	0.1430	0.0982	0.0665	0.0439	0.0279	0.0165	0.0084	0.0026	-0.0014
3.55	0.1421	0.0973	0.0656	0.0430	0.0270	0.0155	0.0075	0.0017	-0.0024
3.50	0.1410	0.0963	0.0645	0.0420	0.0259	0.0145	0.0064	0.0007	-0.0034
3.45	0.1398	0.0951	0.0634	0.0408	0.0247	0.0133	0.0052	-0.0005	-0.0046
3.40	0.1385	0.0938	0.0620	0.0394	0.0234	0.0120	0.0039	-0.0018	-0.0059
3.35	0.1370	0.0922	0.0605	0.0379	0.0219	0.0104	0.0024	-0.0034	-0.0075
3.30	0.1352	0.0904	0.0587	0.0361	0.0201	0.0087	0.0006	-0.0052	-0.0092
3.25	0.1331	0.0884	0.0566	0.0341	0.0180	0.0066	0.0015	-0.0072	-0.0113
3.20	0.1307	0.0860	0.0542	0.0316	0.0156	0.0042	0.0039	-0.0096	-0.0137
3.15	0.1279	0.0831	0.0514	0.0288	0.0127	0.0013	-0.0068	-0.0125	-0.0166
3.10	0.1244	0.0797	0.0480	0.0254	0.0093	-0.0021	-0.0102	-0.0159	-0.0200
3.05	0.1203	0.0756	0.0438	0.0213	0.0052	-0.0062	-0.0143	-0.0200	-0.0241
3.00	0.1153	0.0706	0.0388	0.0162	0.0002	-0.0112	-0.0193	-0.0250	-0.0291
2.95	0.1091	0.0643	0.0326	0.0100	-0.0060	-0.0174	-0.0255	-0.0313	-0.0353
2.90	0.1012	0.0565	0.0247	0.0022	-0.0139	-0.0253	-0.0334	-0.0391	-0.0432
2.85	0.0911	0.0464	0.0147	-0.0079	-0.0240	-0.0354	-0.0435	-0.0492	-0.0533
2.80	0.0779	0.0331	0.0014	-0.0212	-0.0372	-0.0486	-0.0567	-0.0625	-0.0665
2.75	0.0600	0.0152	-0.0165	-0.0391	-0.0551	-0.0666	-0.0746	-0.0804	-0.0845
2.70	0.0349	-0.0098	-0.0416	-0.0642	-0.0802	-0.0916	-0.0997	-0.1054	-0.1095
2.65	-0.0016	-0.0464	-0.0781	-0.1007	-0.1168	-0.1282	-0.1362	-0.1420	-0.1461
2.60	-0.0579	-0.1027	-0.1344	-0.1570	-0.1731	-0.1845	-0.1926	-0.1983	-0.2024

Tab. 1a

ion mass

critical n-value

ELEKTRONENZAHL, GAMMA:
RINGOMETRIE: R, a, b
RHO = 9.551D-01

5.0000D 12 2.700D 01
(CM): 2.300D 00 2.000D-01 2.000D-01

squirrel cage
radius (cm)

squirrel cage radius (cm)	4.00	3.95	3.90	3.85	3.80	3.75	3.70	3.65	3.60	3.55	3.50	3.45	3.40	3.35	3.30	3.25	3.20	3.15	3.10	3.05	3.00	2.95	2.90	2.85	2.80	2.75	2.70	2.65	2.60	2.55	2.50
ringing (clu)	0.2180	0.1546	0.1087	0.0756	0.0518	0.0349	0.0229	0.0143	0.0092	0.0249	0.0139	0.0078	0.0073	0.0073	0.0073	0.0073	0.0073	0.0073	0.0073	0.0073	0.0073	0.0073	0.0073	0.0073	0.0073	0.0073	0.0073	0.0073	0.0073	0.0073	
admittance (squares)	0.2175	0.1542	0.1082	0.0752	0.0514	0.0345	0.0224	0.0139	0.0078	0.0245	0.0139	0.0078	0.0073	0.0073	0.0073	0.0073	0.0073	0.0073	0.0073	0.0073	0.0073	0.0073	0.0073	0.0073	0.0073	0.0073	0.0073	0.0073	0.0073	0.0073	
ion mass	0.2172	0.1538	0.1078	0.0747	0.0510	0.0341	0.0220	0.0134	0.0073	0.0247	0.0134	0.0073	0.0073	0.0073	0.0073	0.0073	0.0073	0.0073	0.0073	0.0073	0.0073	0.0073	0.0073	0.0073	0.0073	0.0073	0.0073	0.0073	0.0073	0.0073	
critical n-value	0.2167	0.1533	0.1073	0.0742	0.0505	0.0336	0.0215	0.0129	0.0069	0.0242	0.0129	0.0069	0.0063	0.0063	0.0063	0.0063	0.0063	0.0063	0.0063	0.0063	0.0063	0.0063	0.0063	0.0063	0.0063	0.0063	0.0063	0.0063	0.0063	0.0063	
1	2	4	8	16	32	64	128	256																							

Tab. 1b

ELEKTRONENZAHL, GAMMA: 5.000D 12 2.700D 01
 RINGOMETRIE: R, a, b (CM): 2.300D 00 1.000D-01 1.000D-01
 RHO = 3.820D 00

1.000D-01 1.000D-01 1.000D-01 1.000D-01 1.000D-01

squirrel cage radius (cm)

	0.4121	0.3010	0.2167	0.1542	0.1086	0.0756	0.0520	0.0350	0.0230
3.95	0.4117	0.3006	0.2163	0.1538	0.1082	0.0752	0.0516	0.0346	0.0226
3.90	0.4113	0.3001	0.2158	0.1533	0.1077	0.0748	0.0511	0.0342	0.0221
3.85	0.4108	0.2996	0.2153	0.1529	0.1073	0.0743	0.0506	0.0337	0.0216
3.80	0.4103	0.2991	0.2148	0.1523	0.1067	0.0738	0.0501	0.0332	0.0211
3.75	0.4097	0.2985	0.2142	0.1517	0.1061	0.0732	0.0495	0.0326	0.0205
3.70	0.4090	0.2978	0.2135	0.1511	0.1055	0.0725	0.0488	0.0319	0.0199
3.65	0.4083	0.2971	0.2128	0.1503	0.1047	0.0718	0.0481	0.0312	0.0191
3.60	0.4074	0.2963	0.2120	0.1495	0.1039	0.0709	0.0473	0.0303	0.0183
3.55	0.4065	0.2953	0.2110	0.1486	0.1030	0.0700	0.0463	0.0294	0.0174
3.50	0.4055	0.2943	0.2100	0.1475	0.1019	0.0690	0.0453	0.0284	0.0163
3.45	0.4043	0.2931	0.2088	0.1464	0.1008	0.0678	0.0441	0.0272	0.0152
3.40	0.4030	0.2918	0.2075	0.1450	0.0994	0.0665	0.0428	0.0259	0.0138
3.35	0.4014	0.2902	0.2059	0.1435	0.0979	0.0649	0.0412	0.0243	0.0123
3.30	0.3997	0.2885	0.2042	0.1417	0.0961	0.0631	0.0395	0.0226	0.0105
3.25	0.3976	0.2864	0.2021	0.1396	0.0940	0.0611	0.0374	0.0205	0.0084
3.20	0.3952	0.2840	0.1997	0.1372	0.0916	0.0587	0.0350	0.0181	0.0060
3.15	0.3923	0.2811	0.1968	0.1344	0.0888	0.0558	0.0321	0.0152	0.0032
3.10	0.3889	0.2777	0.1934	0.1310	0.0854	0.0524	0.0287	0.0118	-0.0002
3.05	0.3848	0.2736	0.1893	0.1268	0.0812	0.0483	0.0246	0.0077	-0.0044
3.00	0.3798	0.2696	0.1843	0.1218	0.0762	0.0432	0.0196	0.0027	-0.0094
2.95	0.3735	0.2624	0.1781	0.1156	0.0700	0.0370	0.0134	-0.0036	-0.0156
2.90	0.3657	0.2545	0.1702	0.1077	0.0621	0.0292	0.0055	-0.0114	-0.0235
2.85	0.3556	0.2444	0.1601	0.0977	0.0521	0.0191	-0.0046	-0.0215	-0.0335
2.80	0.3423	0.2312	0.1469	0.0844	0.0388	0.0058	-0.0178	-0.0348	-0.0468
2.75	0.3244	0.2132	0.1289	0.0665	0.0209	-0.0121	-0.0358	-0.0527	-0.0647
2.70	0.2994	0.1882	0.1039	0.0414	-0.0042	-0.0371	-0.0608	-0.0777	-0.0898
2.65	0.2628	0.1516	0.0673	0.0049	-0.0407	-0.0737	-0.0974	-0.1143	-0.1263
2.60	0.2065	0.0953	0.0110	-0.0514	-0.0970	-0.1300	-0.1537	-0.1706	-0.1826
2.55	0.1131	0.0020	-0.0823	-0.1448	-0.1904	-0.2334	-0.2470	-0.2640	-0.2760
2.50	-0.0588	-0.1700	-0.2543	-0.3167	-0.3623	-0.3953	-0.4190	-0.4359	-0.4479
2.45	-0.4302	-0.5414	-0.6257	-0.6881	-0.7327	-0.7667	-0.7904	-0.8073	-0.8193
2.40	-1.4914	-1.6025	-1.6868	-1.7493	-1.7949	-1.8279	-1.8515	-1.8695	-1.8805

	1	2	4	8	16	32	64	128	256
	1	2	4	8	16	32	64	128	256

Tab. 1c

critical n-value ion mass ($\times 10^3$)

	n _c		100% N ⁺ , without squirrel cage		n (x 10 ³)
300	0	2	4	6	8
200	0	0	0	0	0
180	0	0	0	0	0
160	0	0	0	0	0
140	0	0	0	0	0
120	0	0	0	0	0
110	0	0	0	0	0
80	0	0	0	0	0
60	0	0	0	0	0
40	0	0	0	0	0
20	0	0	0	0	0
18	0	0	0	0	0
17	0	0	0	0	0
16	0	0	0	0	0
15	0	0	0	0	0
14	0	0	0	0	0
13	0	0	0	0	0
12	0	0	0	0	0
11	0	0	0	0	0
10	0	0	0	0	0
9	0	0	0	0	0
8	0	0	0	0	0
7	0	0	0	0	0
6	0	0	0	0	0
5	0	0	0	0	0
4	0	0	0	0	0
3	0	0	0	0	0
2	0	0	0	0	0
1	0	0	0	0	0
0	0	0	0	0	0
300	0	0	0	0	0
200	0	0	0	0	0
180	0	0	0	0	0
160	0	0	0	0	0
140	0	0	0	0	0
120	0	0	0	0	0
100	0	0	0	0	0
80	0	0	0	0	0
60	0	0	0	0	0
40	0	0	0	0	0
20	0	0	0	0	0
18	0	0	0	0	0
17	0	0	0	0	0
16	0	0	0	0	0
15	0	0	0	0	0
14	0	0	0	0	0
13	0	0	0	0	0
12	0	0	0	0	0
11	0	0	0	0	0
10	0	0	0	0	0
9	0	0	0	0	0
8	0	0	0	0	0
7	0	0	0	0	0
6	0	0	0	0	0
5	0	0	0	0	0
4	0	0	0	0	0
3	0	0	0	0	0
2	0	0	0	0	0
1	0	0	0	0	0
0	0	0	0	0	0

Tab. 2a

Tab. 2b

100 % N_2^+ , without squirrel cage

Tab. 2c

	n_c	$n \times 10^3$
300	0	300
200	0	200
180	0	180
160	0	160
140	0	140
120	0	120
100	0	100
80	0	80
60	0	60
40	0	40
20	0	20
18	0	18
17	0	17
16	0	16
15	0	15
14	0	14
13	0	13
12	0	12
11	0	11
10	0	10
9	0	9
8	0	8
7	0	7
6	0	6
5	0	5
4	0	4
3	0	3
2	0	2
1	0	1
0	0	0
300	0.66	300
200	0.66	200
180	0.66	180
160	0.66	160
140	0.66	140
120	0.66	120
100	0.66	100
80	0.66	80
60	0.66	60
40	0.66	40
20	0.66	20
18	0.66	18
17	0.66	17
16	0.66	16
15	0.66	15
14	0.66	14
13	0.66	13
12	0.66	12
11	0.66	11
10	0.66	10
9	0.66	9
8	0.66	8
7	0.66	7
6	0.66	6
5	0.66	5
4	0.66	4
3	0.66	3
2	0.66	2
1	0.66	1
0	0.66	0

 $f \times 10^3$

	n_c	$f \times 10^3$
300	73	300
200	72	200
180	72	180
160	72	160
140	72	140
120	72	120
100	72	100
80	72	80
60	72	60
40	72	40
20	72	20
18	72	18
17	72	17
16	72	16
15	72	15
14	72	14
13	72	13
12	72	12
11	72	11
10	72	10
9	72	9
8	72	8
7	72	7
6	72	6
5	72	5
4	72	4
3	72	3
2	72	2
1	72	1
0	72	0
300	73	300
200	73	200
180	73	180
160	73	160
140	73	140
120	73	120
100	73	100
80	73	80
60	73	60
40	73	40
20	73	20
18	73	18
17	73	17
16	73	16
15	73	15
14	73	14
13	73	13
12	73	12
11	73	11
10	73	10
9	73	9
8	73	8
7	73	7
6	73	6
5	73	5
4	73	4
3	73	3
2	73	2
1	73	1
0	73	0
300	74	300
200	74	200
180	74	180
160	74	160
140	74	140
120	74	120
100	74	100
80	74	80
60	74	60
40	74	40
20	74	20
18	74	18
17	74	17
16	74	16
15	74	15
14	74	14
13	74	13
12	74	12
11	74	11
10	74	10
9	74	9
8	74	8
7	74	7
6	74	6
5	74	5
4	74	4
3	74	3
2	74	2
1	74	1
0	74	0
300	75	300
200	75	200
180	75	180
160	75	160
140	75	140
120	75	120
100	75	100
80	75	80
60	75	60
40	75	40
20	75	20
18	75	18
17	75	17
16	75	16
15	75	15
14	75	14
13	75	13
12	75	12
11	75	11
10	75	10
9	75	9
8	75	8
7	75	7
6	75	6
5	75	5
4	75	4
3	75	3
2	75	2
1	75	1
0	75	0
300	76	300
200	76	200
180	76	180
160	76	160
140	76	140
120	76	120
100	76	100
80	76	80
60	76	60
40	76	40
20	76	20
18	76	18
17	76	17
16	76	16
15	76	15
14	76	14
13	76	13
12	76	12
11	76	11
10	76	10
9	76	9
8	76	8
7	76	7
6	76	6
5	76	5
4	76	4
3	76	3
2	76	2
1	76	1
0	76	0
300	77	300
200	77	200
180	77	180
160	77	160
140	77	140
120	77	120
100	77	100
80	77	80
60	77	60
40	77	40
20	77	20
18	77	18
17	77	17
16	77	16
15	77	15
14	77	14
13	77	13
12	77	12
11	77	11
10	77	10
9	77	9
8	77	8
7	77	7
6	77	6
5	77	5
4	77	4
3	77	3
2	77	2
1	77	1
0	77	0
300	78	300
200	78	200
180	78	180
160	78	160
140	78	140
120	78	120
100	78	100
80	78	80
60	78	60
40	78	40
20	78	20
18	78	18
17	78	17
16	78	16
15	78	15
14	78	14
13	78	13
12	78	12
11	78	11
10	78	10
9	78	9
8	78	8
7	78	7
6	78	6
5	78	5
4	78	4
3	78	3
2	78	2
1	78	1
0	78	0
300	79	300
200	79	200
180	79	180
160	79	160
140	79	140
120	79	120
100	79	100
80	79	80
60	79	60
40	79	40
20	79	20
18	79	18
17	79	17
16	79	16
15	79	15
14	79	14
13	79	13
12	79	12
11	79	11
10	79	10
9	79	9
8	79	8
7	79	7
6	79	6
5	79	5
4	79	4
3	79	3
2	79	2
1	79	1
0	79	0
300	80	300
200	80	200
180	80	180
160	80	160
140	80	140
120	80	120
100	80	100
80	80	80
60	80	60
40	80	40
20	80	20
18	80	18
17	80	17
16	80	16
15	80	15
14	80	14
13	80	13
12	80	12
11	80	11
10	80	10
9	80	9
8	80	8
7	80	7
6	80	6
5	80	5
4	80	4
3	80	3
2	80	2
1	80	1
0	80	0
300	81	300
200	81	200
180	81	180
160	81	160
140	81	140
120	81	120
100	81	100
80	81	80
60	81	60
40	81	40
20	81	20
18	81	18
17	81	17
16	81	16
15	81	15
14	81	14
13	81	13
12	81	12
11	81	11
10	81	10
9	81	9
8	81	8
7	81	7
6	81	6
5	81	5
4	81	4
3	81	3
2	81	2
1	81	1
0	81	0
300	82	300
200	82	200
180	82	180
160	82	160
140	82	140
120	82	120
100	82	100
80	82	80
60	82	60
40	82	40
20	82	20
18	82	18
17	82	17
16	82	16
15	82	15
14	82	14
13	82	13
12	82	12
11	82	11
10	82	10
9	82	9
8	82	8
7	82	7
6	82	6
5	82	5
4	82	4
3	82	3
2	82	2
1	82	1
0	82	0
300	83	300
200	83	200
180	83	180
160	83	160
140	83	140
120	83	120
100	83	100
80	83	80
60	83	60
40	83	40
20	83	20
18	83	18
17	83	17
16	83	16
15	83	15
14	83	14
13	83	13
12	83	12
11	83	11
10	83	10
9	83	9
8	83	8
7	83	7
6	83	6
5	83	5
4	83	4
3	83	3
2	83	2
1	83	1
0	83	0

 $f \times 10^3$

	n

$f(x \times 10^3)$

$-20-26-22-18-16-12-10-8-6-4-2$ $0-2-4-6-8-10-12-14-16-18-20-22-24-26-28-30-32-34-36-38-40-42-44-46$ $(\times 10^3)$

三

100% N⁺ with squirrel cage

Tab. 3a

$f \times 10^3$)

$\pi \times 10^3$

Tab. 3c

100 % N₂⁺, with squirrel cage

Tab. 4a

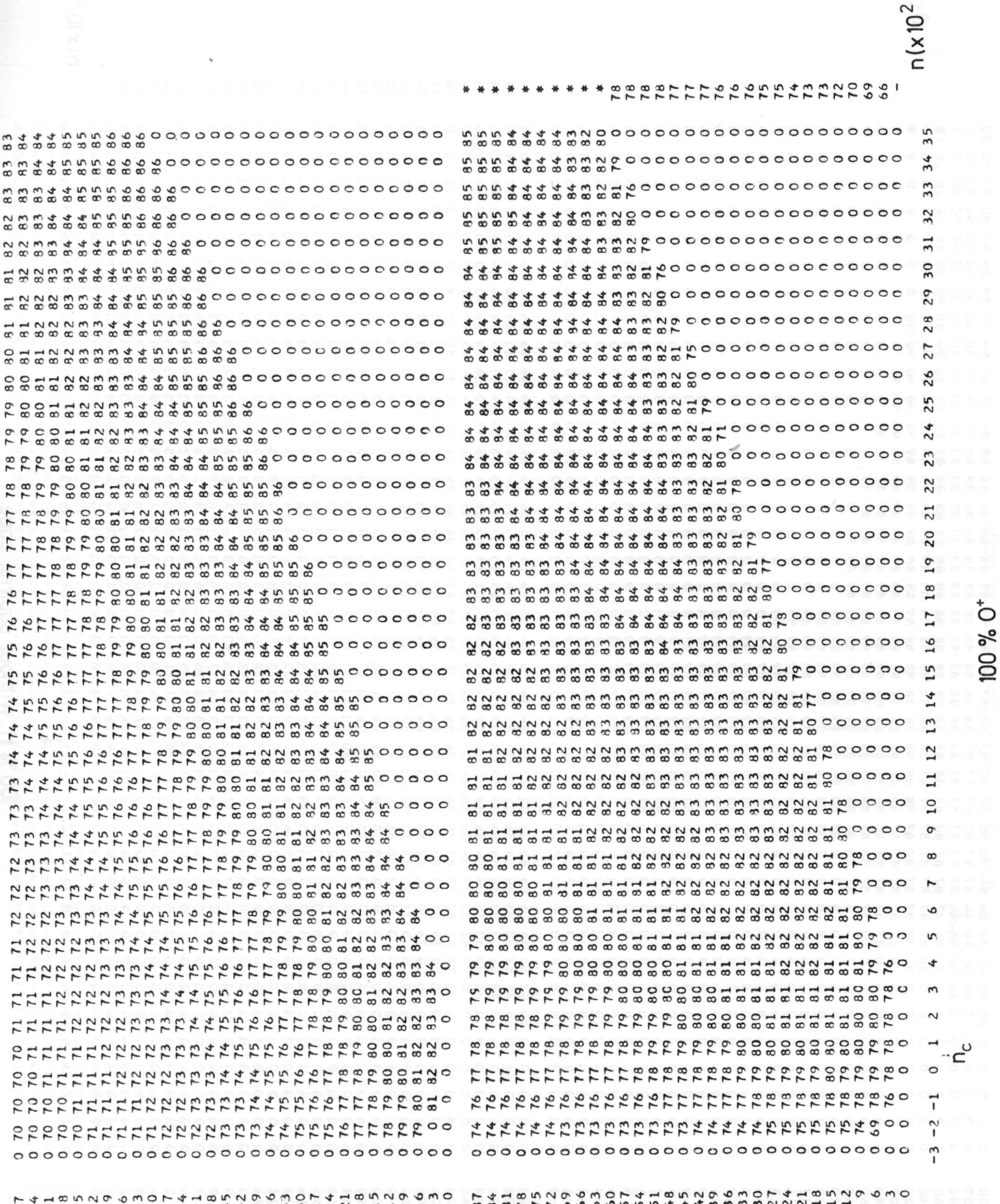
2

Tab. 4b

Tab. 4 c
 n_c
 100 % O⁺ without squirrel cage

f (x^{10²})

Tab. 5b



$f \times 10^2$

100 % H⁺; without squirrel cage

Tab. 6a

f (x 10³)

Tab 6b

n_c	100 % He ⁺ without squirrel cage	$n \times 10^2$
0	0	0
1	0	0
2	0	0
3	0	0
4	0	0
5	0	0
6	0	0
7	0	0
8	0	0
9	0	0
10	0	0
11	0	0
12	0	0
13	0	0
14	0	0
15	0	0
16	0	0
17	0	0
18	0	0
19	0	0
20	0	0
21	0	0
22	0	0
23	0	0
24	0	0
25	0	0
26	0	0
27	0	0
28	0	0
29	0	0
30	0	0
31	0	0
32	0	0
33	0	0
34	0	0
35	0	0
36	0	0
37	0	0
38	0	0
39	0	0
40	0	0
41	0	0
42	0	0
43	0	0
44	0	0
45	0	0
46	0	0
47	0	0
48	0	0
49	0	0
50	0	0
51	0	0
52	0	0
53	0	0
54	0	0
55	0	0
56	0	0
57	0	0
58	0	0
59	0	0
60	0	0
61	0	0
62	0	0
63	0	0
64	0	0
65	0	0
66	0	0
67	0	0
68	0	0
69	0	0
70	0	0
71	0	0
72	0	0
73	0	0
74	0	0
75	0	0
76	0	0
77	0	0
78	0	0
79	0	0
80	0	0
81	0	0
82	0	0
83	0	0
84	0	0
85	0	0
86	0	0
87	0	0
88	0	0
89	0	0
90	0	0
91	0	0
92	0	0
93	0	0
94	0	0
95	0	0
96	0	0
97	0	0
98	0	0
99	0	0
100	0	0
101	0	0
102	0	0
103	0	0
104	0	0
105	0	0
106	0	0
107	0	0
108	0	0
109	0	0
110	0	0
111	0	0
112	0	0
113	0	0
114	0	0
115	0	0
116	0	0
117	0	0
118	0	0
119	0	0
120	0	0
121	0	0
122	0	0
123	0	0
124	0	0
125	0	0
126	0	0
127	0	0
128	0	0
129	0	0
130	0	0
131	0	0
132	0	0
133	0	0
134	0	0
135	0	0
136	0	0
137	0	0
138	0	0
139	0	0
140	0	0
141	0	0
142	0	0
143	0	0
144	0	0
145	0	0
146	0	0
147	0	0
148	0	0
149	0	0
150	0	0
151	0	0
152	0	0
153	0	0
154	0	0
155	0	0
156	0	0
157	0	0
158	0	0
159	0	0
160	0	0
161	0	0
162	0	0
163	0	0
164	0	0
165	0	0
166	0	0
167	0	0
168	0	0
169	0	0
170	0	0
171	0	0
172	0	0
173	0	0
174	0	0
175	0	0
176	0	0
177	0	0
178	0	0
179	0	0
180	0	0
181	0	0
182	0	0
183	0	0
184	0	0
185	0	0
186	0	0
187	0	0
188	0	0
189	0	0
190	0	0
191	0	0
192	0	0
193	0	0
194	0	0
195	0	0
196	0	0
197	0	0
198	0	0
199	0	0
200	0	0
201	0	0
202	0	0
203	0	0
204	0	0
205	0	0
206	0	0
207	0	0
208	0	0
209	0	0
210	0	0
211	0	0
212	0	0
213	0	0
214	0	0
215	0	0
216	0	0
217	0	0
218	0	0
219	0	0
220	0	0
221	0	0
222	0	0
223	0	0
224	0	0
225	0	0
226	0	0
227	0	0
228	0	0
229	0	0
230	0	0
231	0	0
232	0	0
233	0	0
234	0	0
235	0	0
236	0	0
237	0	0
238	0	0
239	0	0
240	0	0
241	0	0
242	0	0
243	0	0
244	0	0
245	0	0
246	0	0
247	0	0
248	0	0
249	0	0
250	0	0
251	0	0
252	0	0
253	0	0
254	0	0
255	0	0
256	0	0
257	0	0
258	0	0
259	0	0
260	0	0
261	0	0
262	0	0
263	0	0
264	0	0
265	0	0
266	0	0
267	0	0
268	0	0
269	0	0
270	0	0
271	0	0
272	0	0
273	0	0
274	0	0
275	0	0
276	0	0
277	0	0
278	0	0
279	0	0
280	0	0
281	0	0
282	0	0
283	0	0
284	0	0
285	0	0
286	0	0
287	0	0
288	0	0
289	0	0
290	0	0
291	0	0
292	0	0
293	0	0
294	0	0
295	0	0
296	0	0
297	0	0
298	0	0
299	0	0
300	0	0
301	0	0
302	0	0
303	0	0
304	0	0
305	0	0
306	0	0
307	0	0
308	0	0
309	0	0
310	0	0
311	0	0
312	0	0
313	0	0
314	0	0
315	0	0
316	0	0
317	0	0
318	0	0
319	0	0
320	0	0
321	0	0
322	0	0
323	0	0
324	0	0
325	0	0
326	0	0
327	0	0
328	0	0
329	0	0
330	0	0
331	0	0
332	0	0
333	0	0
334	0	0
335	0	0
336	0	0
337	0	0
338	0	0
339	0	0
340	0	0
341	0	0
342	0	0
343	0	0
344	0	0
345	0	0
346	0	0
347	0	0
348	0	0
349	0	0
350	0	0
351	0	0
352	0	0
353	0	0
354	0	0
355	0	0
356	0	0
357	0	0
358	0	0
359	0	0
360	0	0
361	0	0
362	0	0
363	0	0
364	0	0
365	0	0
366	0	0
367	0	0
368	0	0
369	0	0
370	0	0
371	0	0
372	0	0
373	0	0
374	0	0
375	0	0
376	0	0
377	0	0
378	0	0
379	0	0
380	0	0
381	0	0
382	0	0
383	0	0
384	0	0
385	0	0
386	0	0
387	0	0
388	0	0
389	0	0
390	0	0
391	0	0
392	0	0
393	0	0
394	0	0
395	0	0
396	0	0
397	0	0
398	0	0
399	0	0
400	0	0
401	0	0
402	0	0
403	0	0
404	0	0
405	0	0
406	0	0
407	0	0
408	0	0
409	0	0
410	0	0
411	0	0
412	0	0
413	0	0
414	0	0
415	0	0
416	0	0
417	0	0
418	0	0
419	0	0
420	0	0
421	0	0
422	0	0
423	0	0
424	0	0
425	0	0
426	0	0
427	0	0
428	0	0
429	0	0
430	0	0
431	0	0
432	0	0
433	0	0
434	0	0
435	0	0
436	0	0
437	0	0
438	0	0
439	0	0
440	0	0
441	0	0
442	0	0
443	0	0
444	0	0
445	0	0
446	0	0
447	0	0
448	0	0
449	0	0
450	0	0
451	0	0
452	0	0
453	0	0
454	0	0
455	0	0
456	0	0
457	0	0
458	0	0
459	0	0
460	0	0
461	0	0
462	0	0
463	0	0
464	0	0
465	0	0
466	0	0
467	0	0
468	0	0
469	0	0
470	0	0
471	0	0
472	0	0
473	0	0
474	0	0
475	0	0
476	0	0
477	0	0
478	0	0
479	0	0
480	0	0
481	0	0
482	0	0
483	0	0
484	0	0
485	0	0
486	0	0
487	0	0
488	0	0
489	0	0
490	0	0
491	0	0
492	0	0
493	0	0
494	0	0
495	0	0
496	0	0
497	0	0
498	0	0
499	0	0
500	0	0
501	0	0
502	0	0
503	0	0
504	0	0
505	0	0
506	0	0
507</		

Tab. 6c

Tab. 7a

Tab. 7b

300

$$f(x \times 10^3)$$

78

100% He⁺, with squirrel cage

Tab.8: GROWTH OF INSTABILITY Comparison of selected data

sum of fractional loadings	100%	50%	0%	N^+
	0%	50%	100%	N_2^+
1%	61	60	60	with SQC
2%	64	63	63	
1%	61	61	60	without
2%	65	64	63	

	100%	50%	0%	N^+
	0%	50%	100%	O^+
3%	66	66	66	with SQC
15%	73	73	73	
45%	78	78	77	without
3%	66	66	66	
15%	73	73	73	
45%	78	78	78	

	100%	50%	0%	H^+
	0%	50%	100%	He^+
1%	67	65	64	with SQC
2%	70	69	67	
4%	73	72	70	without
10%	77	76	74	
20%	80	79	77	
1%	67	66	64	
2%	70	69	67	
4%	73	72	70	
10%	77	76	74	
20%	80	79	77	